ACS OMEGA

Open Access

http://pubs.acs.org/journal/acsodf

Article

Utilization of *Ananas comosus* Crown Residue Husk as a Sustainable Strength Additive for EPR/LDPE Blend Composites

Jitendra Kumar, Anuj Kumar, Atul Kumar Maurya, Hariome Sharan Gupta, Surendra Pal Singh, and Chhaya Sharma*

Cite This: *ACS Omega* 2024, 9, 2740−2751

Read Online

ACCESS | Metrics & More | Article Recommendations

ABSTRACT: The utilization of waste generated by natural resources is a crucial problem nowadays. The current study describes the utilization of pineapple (*Ananas comosus*) crown residue husk (PCRh) as a strength additive for low-density polyethylene (LDPE) and ethylene propylene rubber (EPR) composites. The blend composites with 30% husk, 10 wt % EPR, and 60% LDPE content showed much better mechanical properties, such as tensile strength and flexural properties, than pristine LDPE and its binary composite with 10 wt % EPR. The high tensile strength (∼19.28 MPa) and tensile modulus (522.97 MPa) were obtained for the composite consisting of 30 wt % PCRh in the basic polymer matrix. Similarly, the highest flexural strength (∼18.09 MPa) and modulus (∼790.29 MPa) were recorded for the same composition. The incorporation of PCRh with LDPE and EPR was further characterized by attenuated total reflection−Fourier transform infrared, differential scanning calorimetry, field emission scanning electron microscopy, dynamic mechanical analysis, and a universal testing machine to evaluate its impact on various properties.

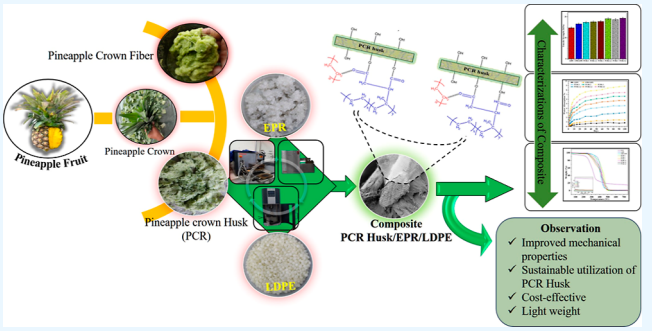

1. INTRODUCTION

Polymer composites are now widely used in various industries, including transportation, the aerospace industry, and packaging,[1−4] attributable to their excellent corrosion resistance, low density, translucency, and high stiffness.[5,6] Polymer composites reinforce natural fibers to improve their mechanical and electrical characteristics. These natural fibers are nontoxic, biodegradable, readily available, and light in weight.[7,8] As a result, they are widely used to create polymer composites that are reinforced with fiber. Natural fibers like jute, cotton, hemp, sisal, date palm leaf coir, flax, sawdust, and rice husk are frequently used in polymer composites.[4,9−15] Natural fibers are a great alternative to synthetic reinforcements because of their widespread availability and flexibility in improving their qualities via surface treatments.[16−18] These composites are used in the construction and automotive industries.[1,3,6,19] Several studies reported using a variety of thermoplastic polymers for reinforcing natural fiber using polypropylene, santoprene, low-density polyethylene (LDPE), HDPE, and polyvinyl chloride.[1,2,20,21]

Automotive manufacturers are increasing demand for natural polymer composites that can minimize pollution while still being lighter and more fuel efficient.[3−5] Natural fibers are more shatter resistant than glass fiber composites, have enhanced energy management capabilities, and have higher sound absorption efficiency.[2,6] Such composites minimize the weight of vehicle components by 80% while reducing the energy required for manufacture.[2] By substitution of different kinds of lignocellulose fibers for glass fibers, environmentally friendly composites may be created. Demand for natural fibers in plastic composites is anticipated to increase by 15−20% yearly, with growth rates of 15−20% in automotive applications and 50−80% in a few specific construction applications.[2] Industrial and consumer products, including tiles, garden tools, plant pots, furniture, and oceanic piers, are some of the other expanding markets.[2,3,6−13]

Additionally, there is a renewal of interest in researching more ecologically friendly materials due to the ongoing environmental issues. As a result, problems such as biodegradability and protection of the environment became critical to address while looking at novel materials. A theory increasingly used in most study sectors, sustainable development or eco-design, is often employed while creating new

Received: October 6, 2023
Revised: November 23, 2023
Accepted: November 24, 2023
Published: January 4, 2024

https://doi.org/10.1021/acsomega.3c07697
ACS Omega 2024, 9, 2740−2751

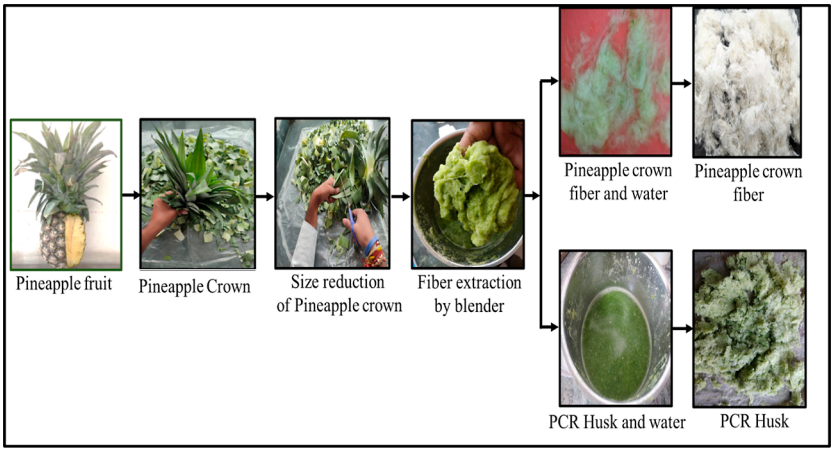

Figure 1. Extraction procedure of PCR husk from pineapple crown. (Photograph courtesy of "Jitendra Kumar". Copyright 2023.)

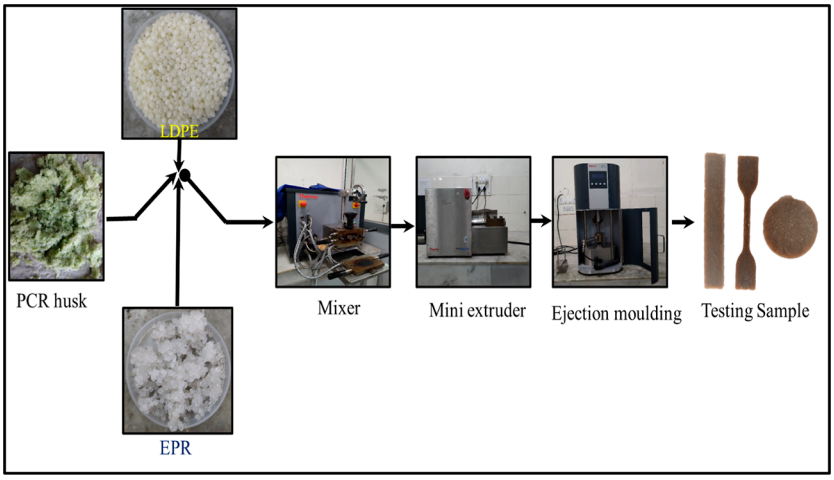

Figure 2. Polymer composite and testing specimen made from PCRh. (Photograph courtesy of "Jitendra Kumar". Copyright 2023.)

goods. The farming sector directly or indirectly relies on the environment as a source of raw materials for its growth and places to "dumpsites" for trash and byproducts produced throughout the production cycles. Pineapple is one of the sources of these raw materials, but it generates plenty of waste, and its utilization may be done by finding its potential applications. The high cellulose content of pineapple fibers ensures that the fibers have high mechanical properties (tensile and flexural).[14,15] The annual harvest of pineapples is 28.18 million metric tonnes (MMT), with India producing 1.706 MMT of pineapples, ranking sixth in the world.[16] These fibers have been used in paper, textiles, polymer composites, nitrocellulose,[1,3,17−19,22−24] and polymer composites. In the literature, pineapple crown fibers have previously been documented to be used in polymeric composites. However, PCRh remains after the extraction of the pineapple crow fiber. The PCRh utilization, mainly as reinforcement, is still in its formative stages. As can be observed from the previous literature review, natural fibers like rice husk[25,26] or sawdust[27,28] have been successfully used as an additive material for creating polymer matrix composites. The combination of the PCRh and LDPE polymer and blend with ethylene propylene rubber (EPR) was added as a compatibilizer to develop a blend polymer composite material.

Similarly, PCRh/LDPE and PCRh/EPR/LDPE blend systems, where EPR was mixed in 10 wt % quantities, were comparatively investigated in this study. This work is done in continuation of our previous work25 and primarily studies the interaction of PCRh with EPR/LDPE polymer blends. Apart from this, the influence of the addition of PCRh on the crystallization and thermal behavior of the different polymers in the blends was also studied. Maleic anhydride (MAH)-grafted EPR was introduced to compare the properties of PCRh/LDPE polymer composites when one of the polymer phases (LDPE) is replaced with its functionalized EPR/LDPE blend. The morphologies, thermal stabilities, and mechanical properties of the polymer composite and blend composites were also investigated and found to be very reliable to apply in real applications.

2. EXPERIMENTAL SECTION

2.1. Materials. LDPE, marketed as RELENE 24FS040, was purchased from Reliance Industry Limited in India. It has a density of 0.922 g cm^{-3} and a melt flow index of 4.0 g/10 min. ExxonMobil Chemical Asia Pacific received EPR from Singapore as a marketed product. Exxelor VA 1803 is grafted with 0.75% MAH (density −0.86 g cm^{-3} and melt flow index −3.3 g/10 min (230 °C/2.16 kg).

2.2. Extraction of PCRh. Pineapple fruit waste (crown) was collected from a local juice vendor in Saharanpur, Uttar Pradesh (India). The dust particles on the surfaces of the crown were removed by washing the crown with distilled

https://doi.org/10.1021/acsomega.3c07697
ACS Omega 2024, 9, 2740−2751

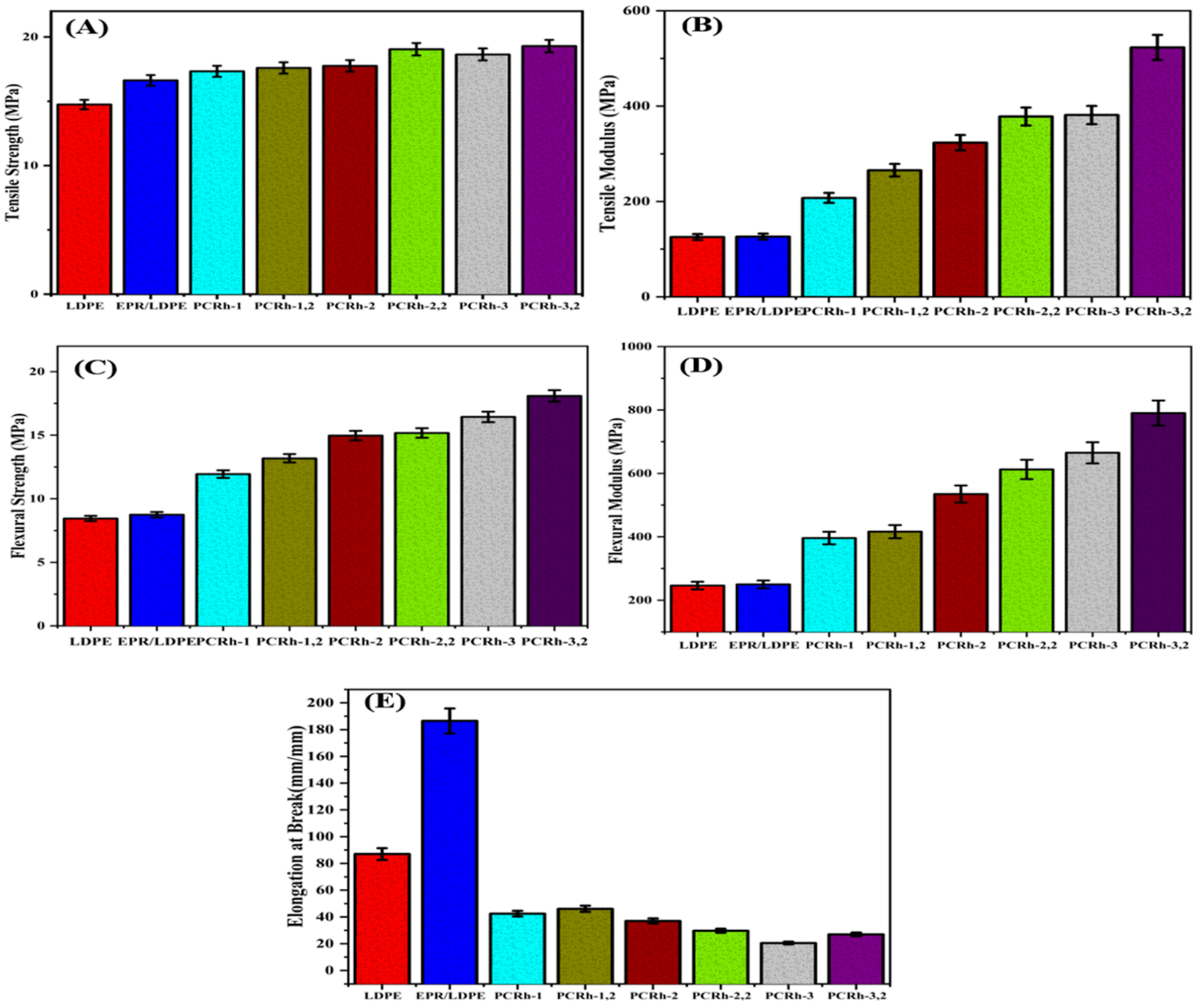

Figure 3. Tensile strength (A), tensile modulus (B), flexural strength (C), flexural modulus (D), and elongation at break (E) of all polymer composites of PCRh/EPR/LDPE.

water. After that, the crown was chopped into small pieces (typically 8−10 mm lengths) to extract PCRh, which was extracted using a blender at 12,000−15,000 rpm, as shown in Figure 1. Thereafter, light green PCRh (size ≤450 μm) was dried at 60 °C for 48 h.

2.2.1. LDPE/EPR Blend Mixing and Composite Making with PCR Husk. The PCRh blend polymer composite was produced by mixing with the different ratios of PCRh (10/90, 20/80, and 30/70 PCRh/LDPE and 10/10/80, 20/10/70, and 30/10/60 wt % PCRh/EPR/LDPE) blended in a Thermo Scientific Haake Rheomix machine at 50 rpm at a temperature of 160 °C for 10 min[29] The PCRh blend composite samples were subsequently left to cool for 10 min at room temperature.

2.2.2. Sample Preparation. Lumps of the composites were dried before further processing. The melting process was reiterated, and the material was extruded into the HAAKE Rheomex mini CTW twin screw mixer made by Thermo Fisher SCIENTIFIC. The temperature of Thermo Scientific's HAAKE Minijet II machine was kept at 160 °C with 550 bar injection pressure and then filled with these melts of the composites. The samples were prepared following tensile ISO 5272-2 and flexural ISO 178:2019 standards, and the procedure is shown in Figure 2.

2.3. Characterization. *2.3.1. Universal Testing Machine.* The tensile strength and modulus of the samples were determined using a universal testing machine (UTM, model 3365, INSTRON 5KN). The tensile properties of different composites with and without a compatibilizer were tested at room temperature and a crosshead speed of 15 mm/min, following ISO 527-2. Here, the results of an average of five tests on each sample are provided. Additionally, all the composite samples' flexural strength was evaluated using the same UTM following the ISO 178:2019 standard at room temperature with a reduced crosshead speed of 2 mm/min. The experiments were repeated five times for each sample, and its average was reported.

2.3.2. Field Emission Scanning Electron Microscopy. The original LDPE and all composite morphologies were examined by a field emission scanning electron microscope (model Mira3 Tescan). All of the composite samples were covered with a thin coating of gold for field emission scanning electron microscopy (FE-SEM) pictures. The polymer matrix covered

https://doi.org/10.1021/acsomega.3c07697
ACS Omega 2024, 9, 2740−2751

Table 1. Sample Nomenclature and Various Properties of Different Composites Made from PCR with LDPE/EPR[a]

LDPE	PCRh	EPR	sample naming	T.S. (MPa) ±SD	T.M. (MPa) ±SD	% elongation ±SD	F.S. (MPa) ±SD	F.M. (MPa) ±SD
100	0	0	LDPE	14.74 ± 0.37	125.42 ± 6.27	87.03 ± 4.35	8.44 ± 0.21	245.79 ± 12.29
90	10	0	PCRh-1	17.32 ± 0.43	207.45 ± 10.37	42.50 ± 2.12	11.94 ± 0.30	396.05 ± 19.80
80	20	0	PCRh-2	17.75 ± 0.44	323.18 ± 16.15	37.06 ± 1.85	14.97 ± 0.33	534.94 ± 26.74
70	30	0	PCRh-3	18.64 ± 0.46	381.10 ± 19.05	20.55 ± 1.02	16.44 ± 0.41	664.81 ± 33.24
90	0	10	EPR/LDPE	16.61 ± 0.41	126.20 ± 6.31	186.49 ± 9.32	8.74 ± 0.22	249.49 ± 12.47
80	10	10	PCRh-1,2	17.59 ± 0.43	265.43± 13.27	46.11 ± 2.30	13.17 ± 0.32	416.28 ± 20.81
70	20	10	PCRh-2,2	19.04 ± 0.47	378.24 ± 18.91	29.72 ± 1.49	15.17 ± 0.37	612.42 ± 30.62
60	30	10	PCRh-3,2	19.28 ± 0.48	522.97 ± 26.14	26.94 ± 0.55	18.09 ± 0.45	790.29 ± 39.51

[a]T.M.—Tensile modulus, F.M.—flexural modulus, T.S.—Tensile strength, F.S.—flexural strength, S.D.—standard deviation. The variation of different parameters is shown in Figure 3.

PCRh in every picture, obtained with the same resolution and an accelerating scanning voltage of 10 kV.

2.3.3. Attenuated Total Reflection–Fourier Transform Infrared. To investigate the change in the functional groups due to chemical interactions between the polymer matrix and PCRh, attenuated total reflection–Fourier transform infrared (ATR–FTIR) data was collected by a PerkinElmer Spectrum 2 Instrument in accordance with ASTM D5576-00(2013) standards. The ATR–FTIR spectrometer range was employed at 4000–400 cm^{-1}.

2.3.4. Dynamic Mechanical Analysis. Testing all composites according to ASTM D5023-15, a thermomechanical analysis was conducted in a NETZSCH dynamic mechanical analysis (DMA) setup at temperatures between −60 and 150 °C, with 4 °C/min heating rate at 1 Hz frequency. The analysis's storage modulus (E') and tan δ results have been plotted as a function of temperature.

2.3.5. Wide-Angle X-ray Diffraction. In order to accurately examine the crystalline structure, the samples of virgin LDPE, EPR/LDPE blend matrix, and PCRh composites were dried at 60 °C for 24 h to reduce the moisture content. Wide-angle X-ray diffraction (Rigaku Ultima IV) was employed for this purpose using Cu K with nickel filtering as the radiation source (λ = 0.15406 nm). The diffraction patterns were acquired in the 2θ range of 5–80° with a 4°/min scanning rate.

2.3.6. Thermogravimetric Analysis. Approximately 10 mg of the composites, virgin LDPE, and EPR/LDPE blend matrix was taken in an Extar TG/DTA apparatus. 200 mL/min of nitrogen gas (N_2) was supplied to generate the inert environment. The heating rate was kept constant throughout the experiment at 10 °C/min. In accordance with the ASTM E1131-08 (2014) standard, the temperature range was put to 35–800 °C.

2.3.7. Differential Scanning Calorimetry. Differential scanning calorimetry (DSC) was performed using a DSC 25, TA Instruments. The sample was heated between 60 and 150 °C with a heating rate of 5 °C/min under an environment of nitrogen. The second cycle's melting and crystallization data were always taken into consideration. About 10 mg of the substance was heated in an uncovered aluminum sample pan, with the empty pan as a reference. Equation 1 was used to determine the fractional crystallinity of all composites.

$$x_C = \frac{\Delta H_m \times 100}{W_m \times \Delta H_m^0} \quad (1)$$

where ΔH_m^0 = 285 J g^{-1}, the heat of fusion for 100% crystalline LDPE, ΔH_m is the melting enthalpies, and W_m is the weight fraction of the polymeric matrix in the composite.

2.3.8. Water Absorption Test. The investigations of water absorption and thickness swelling were made for the composite of PCRh with a polymeric matrix (EPR/LDPE) in accordance with ASTM D 570-98. Samples were dried at 80 °C for 1 h using a hot air vacuum oven to get them free of moisture. Following this, the samples were cooled in a desiccator, weighed to three decimal places, and then immediately placed in distilled water. The thickness and weight of the submerged samples were measured for 100 days. Samples submerged in distilled water were cleaned using a clean towel or tissue paper to assess their weight and thickness.[15,30,31] eq 2 was used to determine changes in weight gain percentage and swelling of thickness percentage by eq 3.

$$\text{Water uptake (\%)} = \frac{W_{wet} - W_{dry}}{W_{wet}} \times 100 \quad (2)$$

where W_{wet} is the weight of the soaked sample and W_{dry} is the initial weight of the sample prior to its immersion in distilled water.

$$\text{Thickness swelling (\%)} = \frac{t_{wet} - t_{dry}}{t_{wet}} \times 100 \quad (3)$$

where t_{wet} is the thickness of the soaked samples and t_{dry} is the initial thickness of the sample in the dry state.

3. RESULTS AND DISCUSSION

The various mechanical properties such as tensile strength, tensile modulus, % elongation, flexural modulus, and flexural strength are investigated for composites having different ratios of polymer matrix and PCRh. The values of these properties are listed in Table 1. In the pristine LDPE case, the tensile strength value was observed at 14.74 MPa. However, it increased to 18.64 after the addition of 30% PCRh. Similarly, the tensile strength of the EPR/LDPE composite was observed at 16.61 MPa, which is higher than that of the PCRh/LDPE composite. In view of this, various composites of EPR/LDPE up to 30% PCRh were made, and their properties were investigated. The PCRh ratio was limited to 30% due to no proper mixing with the polymer matrix beyond this ratio. At this ratio, a tremendous increase in the tensile strength can be seen, as shown in Table 1 for PCRh-3,2. A similar trend was observed for tensile modulus, flexural strength, and flexural modulus in the case of all of the composites. However, the value of % elongation was decreased from LDPE to PCRh-3 and increased for EPR/LDPE composite due to the addition of EPR. In the case of PCRh-3,2 composite, a rapid decrease in % elongation was observed. Hence, the proliferation of PCRh

https://doi.org/10.1021/acsomega.3c07697
ACS Omega 2024, 9, 2740–2751

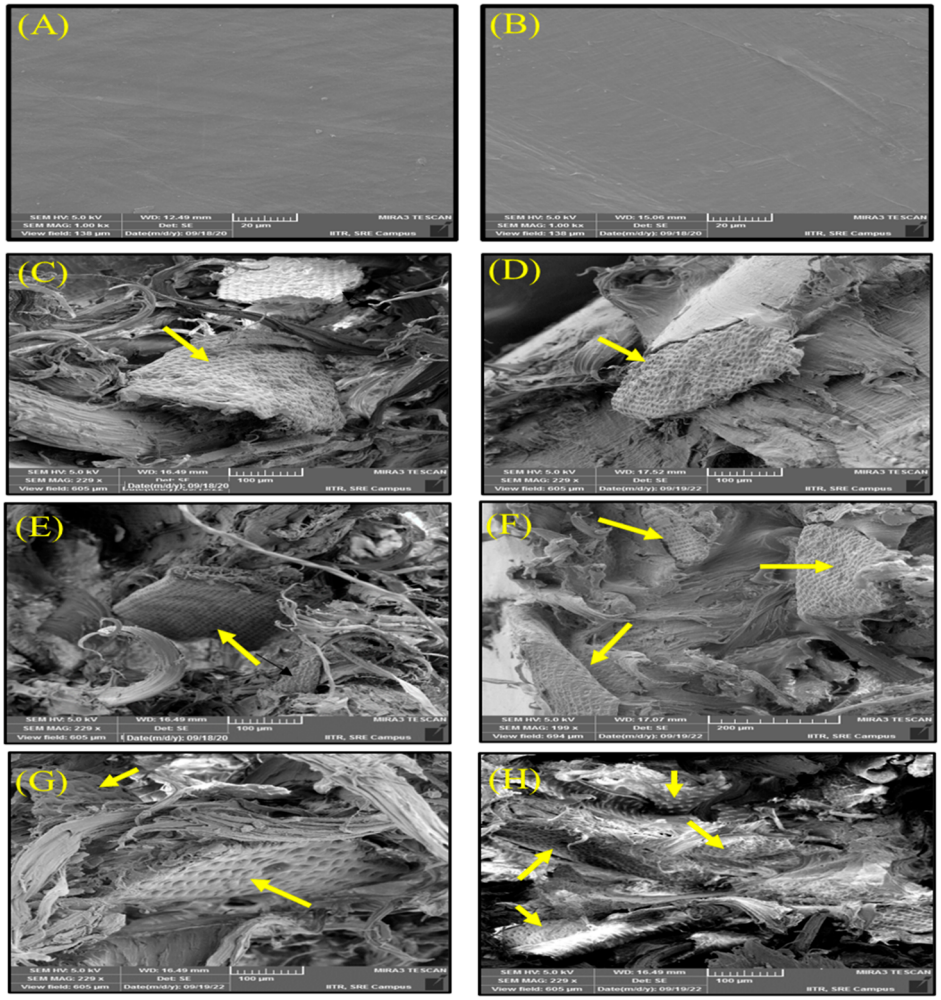

Figure 4. FE-SEM images of (A) virgin LDPE matrix, (B) EPR/LDPE blend matrix, (C) PCRh-1, (E) PCRh-2, (G) PCRh-3 and blend composite, (D) PCRh-1,2, (F) PCRh-2,2, and (H) PCRh-3,2.

played a crucial role in the variation of the different mechanical properties of the polymer matrix.

3.1. Characterization. In order to evaluate the compatibility and characteristics of polymer PCRh composites, the diffraction pattern was recorded using XRD, and FE-SEM determined the morphological properties.

3.1.1. Field Emission Scanning Electron Microscopy. The SEM images were obtained to observe the morphology and structural changes in the composite. Figure 4A,C,E,G represents the surface morphology of pure LDPE, PCRh-1, PCRh-2, and PCRh-3, whereas Figure 4B,D,F,H represents the surface morphology of EPR/LDPE, PCRh-1,2, PCRh-2,2, and PCRh-3,2. It can be observed from the SEM images that PCRh was compatible with both EPR and LDPE, although some stretching of LDPE was observed in the case of the PCRh/LDPE binary composite (Figure 4C, E, and G—thread-like structure). However, the thread-like structures were not observed in a blended composite with 10% EPR with PCRh and LDPE (Figure 4D, F, and H); hence, the strength properties may also increase as a result of the addition of PCRh. Another contributing factor may be the generation of the voids, observed in the case of PCRh/LDPE composite but not in the case of PCRh/EPR/LDPE composites because the EPR filled these voids, and as a result, it reduced stress concentration. In other words, it leads to a more uniform distribution of stress throughout the material, which results in enhanced strength. Apart from that, EPR has a higher affinity for both PCRh and LDPE than LDPE alone. As a result, it also increases interfacial adhesion, which leads to better load transfer between the different components of the composite and hence the strength,[32−34] corroborating with Figure 4B,F,H.

3.1.2. Attenuated Total Reflection−Fourier Transform Infrared. Figure 5A−D demonstrates the ATR−FTIR spectra of pristine LDPE, LDPE with compatibilizer EPR, virgin PCRh, and the PCRh-3,2 composite. Because of the hydrogen bonding in the biomaterial, PCRh, the FTIR−ATR peak at around 3320 cm^{-1} is related to the O−H stretching. Similar to this, peaks at 2850 and 2924 cm^{-1} represent the C−H symmetric and asymmetric stretching of the aliphatic CH_3 group of cellulose, hemicellulose, and lignin.[35] Moreover, the existence of an aromatic lignin ring was confirmed by the peak at 1733 cm^{-1} corresponding to the C−O stretching vibration. Other peaks, located at 1465, 1371, and 1037 cm^{-1}, respectively, show the existence of the −HCH, C−H bending vibration and the C−O−C asymmetric stretching.[22]

The distinctive peaks at 2925 and 2855 cm^{-1} in Figure 5B of the EPR/LDPE mix represent symmetric and asymmetric C−H alkyl stretch, respectively. Additionally, it presents peaks at 1460, 1377, and 724 cm^{-1}, which are associated with the

https://doi.org/10.1021/acsomega.3c07697
ACS Omega 2024, 9, 2740−2751

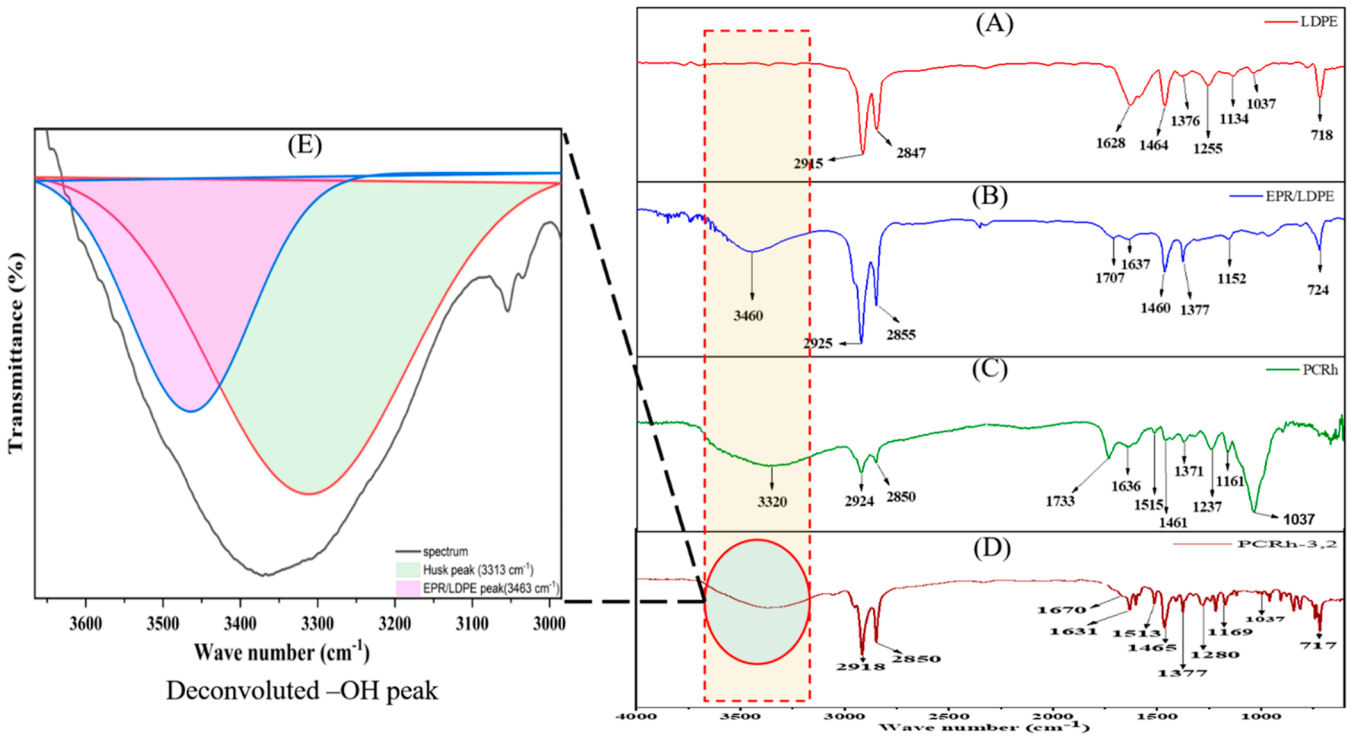

Figure 5. ATR−FTIR of (A) virgin LDPE, (B) EPR/LDPE blend matrix, (C) PCRh, (D) PCRh-3,2, and (E) deconvoluted −OH peak of the spectrum.

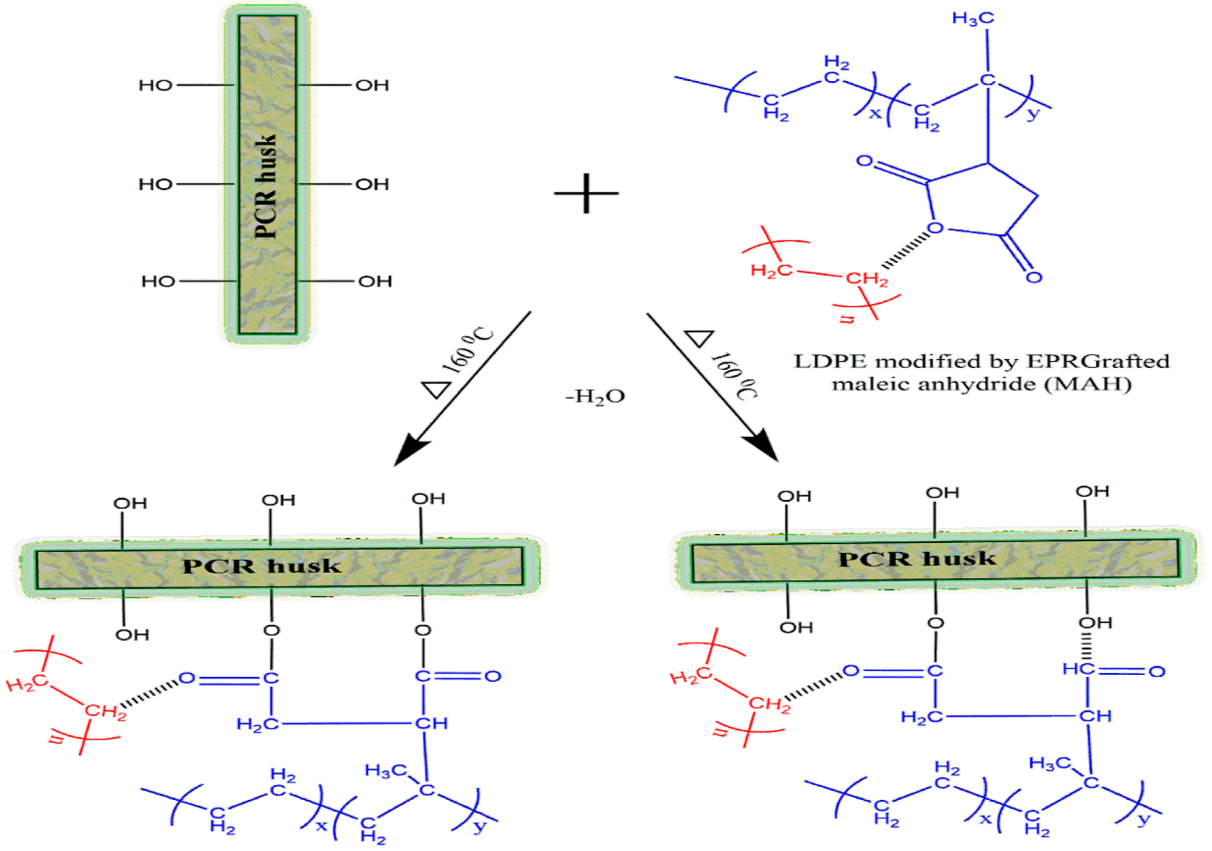

Figure 6. Schematic of ester bond formation between −OH group on the surface of PCRh and MAH group of the EPR.[25] (Adapted with permission from ref 25. Copyright 2022, John Wiley & Sons.)

bending and rocking vibrations of the aliphatic groups CH_2 and CH_3, respectively. The bands at 1790 and 1707 cm^{-1} were observed due to grafting of MAH on EPR of the EPR/LDPE blend composites, which conform to the carbonyl (C−O)

https://doi.org/10.1021/acsomega.3c07697
ACS Omega 2024, 9, 2740−2751

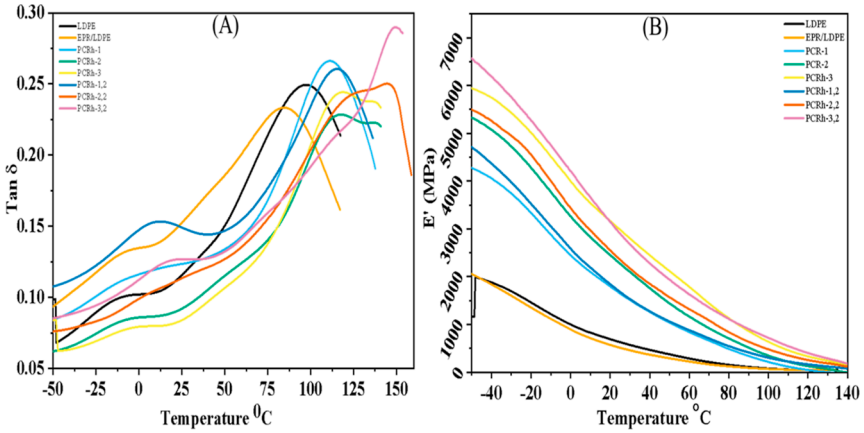

Figure 7. Virgin LDPE, EPR/LDPE blend matrix, and all polymer composites of PCRh/EPR/LDPE graph. (A) Storage modulus and (B) tan δ versus temperature.

asymmetric anhydride stretching band and the C−O symmetric stretching of the carboxylate groups present in maleic acid.[25−27]

Additionally, the existence of CH symmetric and asymmetric vibrations of CH_3 is confirmed by peaks at around 2915 and 2847 cm^{-1} in Figure 5A. Likewise, peaks at 1464, 1376, and 718 cm^{-1} are related to the bending vibrations of the aliphatic groups CH_2 and CH_3, as well as the rocking vibrations of CH_2, which indicate the existence of LDPE.

The PCRh-3,2 composite's ATR-FTIR spectra display two additional distinctive peaks at 1749 and 1631 cm^{-1}. The peak at 1631 cm^{-1} corresponds to the specific peaks of PCRh, although the other peak at 1749 cm^{-1} corresponds to the ester bond formation.[35−37] One small peak next to 2918 cm^{-1} was due to EPR, which confirms the compatibility of EPR in the composite. The specific peak at 1037 cm^{-1} corresponds to the husk itself. The PCRh-3,2 composite showed a broader peak in the region from 3000 to 3600 cm^{-1}, formed due to the hydrogen bond contribution from PCRh alone and the EPR/LDPE composite, as shown by the deconvolution of the peak.[38] On the basis of the above facts, the ester bond formation described in Figure 6 is consistent with the mechanism described by Malkapuram et al.[28] and Kallakas et al.[39]

3.1.3. Dynamic Mechanical Analysis. 3.1.3.1. Storage Modulus. Storage modulus (E') is a measure of the stiffness and rigidity of a material. It is a viscoelastic property, which is significant in natural fiber polymer composites, as it is a key indicator of their performance in applications where they are subjected to dynamic loads. Figure 7A shows E' of LDPE, EPR/LDPE blend, and all composites as a function of the temperature from −50 to 150 °C. Across the entire temperature range, all of the composites exhibited greater E' values than virgin LDPE. LDPE, EPR/LDPE, and all the composites, PCRh-1, PCRh-2, PCRh-3, PCRh-1,2, PCRh-2,2, and PCRh-3,2, reported E′ of 1985, 2052, 4285, 5321, 5949, 4700, 5495, and 6542 MPa, respectively, at a temperature of −50 °C. Due to the inclusion of EPR, which already had a lower storage modulus as compared to LDPE, the EPR/LDPE blend exhibited a storage modulus lower than that of LDPE. It is fascinating to observe that all the composites' storage modulus seemed to rise compared to LDPE and EPR. The inclusion of PCRh in the LDPE and EPR/LDPE blends caused an increase in the storage modulus of each of the composites. Moreover, the interfacial interaction was crucial in improving the composites' modulus characteristics. Likewise, all the composite samples showed a storage modulus of 623, 517, 1643, 2261, 2997, 1687, 2356, and 2902 MPa, respectively, at room temperature (25 °C) for samples LDPE, EPR/LDPE PCRh-1, PCRh-2, PCRh-3, PCRh-1,2, PCRh-2,2, and PCRh-3,2, respectively. Compared to pure LDPE, composites PCRh-1, PCRh-2, PCRh-3, PCRh-1,2, PCRh-2,2, and PCRh-3,2 exhibited an increment of 163.72, 262.92, 381.06, 170.78, 278.17, and 365.81% in the E' values. This apparent increase in the E' of the composites is likely the result of limitations placed on the mobility of the polymeric chains by reinforcing PCRh. Alkali-treated groundnut shell powder-reinforced ABS composites were made by Kumar et al.[29] and Maurya et al.,[12] who also found an increase in the storage moduli of the composites. Similarly, Abdelmouleh et al.[30] reinforced natural rubber and LDPE with silane-treated cellulosic fiber and observed the same impact of a rising trend in storage modulus as a result of the short fiber loading.

3.1.3.2. Damping Factor (tan δ). The tan δ vs temperature curve for LDPE, EPR/LDPE, and all composites is shown in Figure 7B. Glass-transition temperature (T_g) for LDPE is roughly −13.58 °C. T_g values of about −9.33, −5.13, −3.17, 9.20, 11.63, and 17.19 °C were recorded for PCRh-1, PCRh-2, PCRh-3, PCRh-1,2, PCRh-2,2, and PCRh-3,2 respectively. It is interesting to note that every blend recorded a T_g value higher than the pure LDPE. This increase in T_g resulted from the PCRh limitation of the LDPE and EPR/LDPE matrices' chain mobility. The present assertion agreed with the information provided by Kumar et al. and Maurya et al.[13,25] Additionally, the T_g values of all the composites may have been increased compared to pure LDPE owing to a significant interfacial contact caused by the creation of ester and hydrogen bonds at the interface of the PCRh and polymer matrix. PCRh has a large surface area and contains polar hydroxyl groups. These polar groups interact with the polymer chains and restrict their mobility. This restriction in mobility leads to an increase in T_g.[40−42] Apart from that, PCRh forms strong interfacial bonds with the polymer matrix through chemical and physical interactions. These strong bonds help to transfer stress between the husk and the matrix, which further restricts polymer chain mobility and increases T_g.[41,43,44]

3.1.4. XRD. The XRD pattern was recorded for all of the prepared samples to observe the changes in the crystallinity. Five characteristic peaks labeled (a−e) were observed in the XRD pattern of blend composites. The crystallinity was

https://doi.org/10.1021/acsomega.3c07697
ACS Omega 2024, 9, 2740−2751

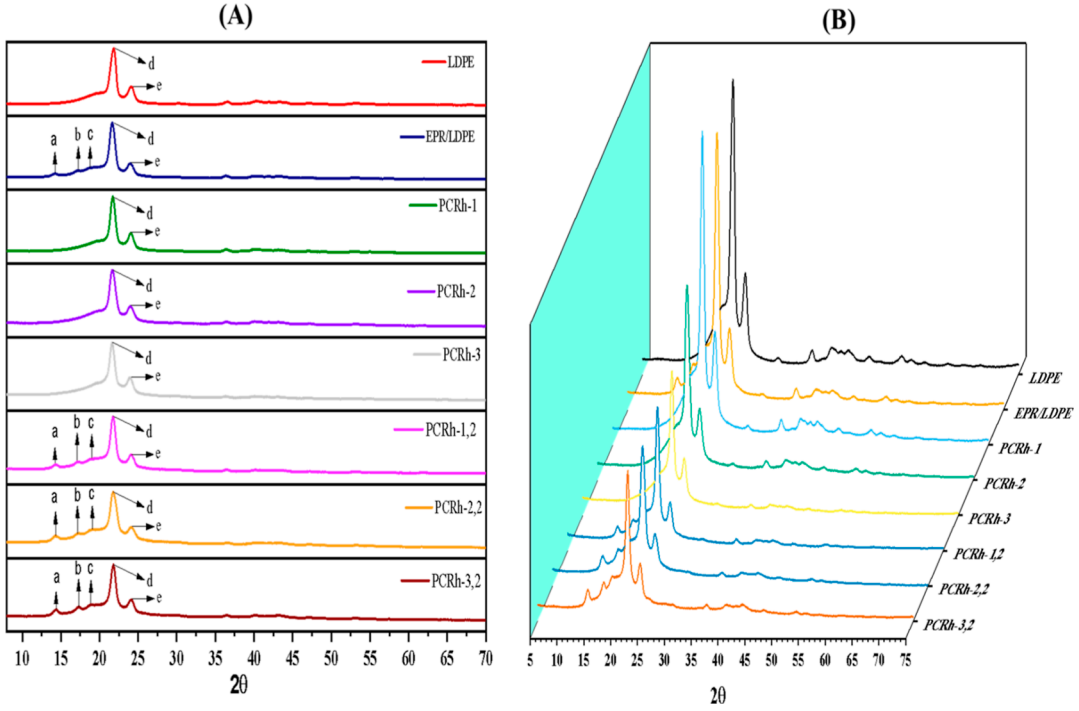

Figure 8. (A) XRD pattern of virgin LDPE. EPR/LDPE blend matrix and all various composites and (B) their 3D representation for intensity comparison of the peaks.

maintained for PCRh-1,2, PCRh-2,2, and PCRh-3,2, as depicted in Figure 8, but the reduction in the intensity of the peaks d and e can be seen, probably due to a gradual decrease in the addition of LDPE concentration. This statement is corroborated with the DSC data provided in Table 3.

Table 2. TGA Data Showing the Onset Temperatures with Respective Weight Loss (%)[a]

sample	T_i (°C)	T_{50} (°C)	T_{75} (°C)	T_{max} (°C)
PCRh	213.54	327.84	617.28	794.69
LDPE	327.04	422.62	437.62	509.92
EPR/LDPE	325.88	406.79	426.36	511.84
PCRh-1	304.04	437.84	455.91	523.29
PCRh-2	276.91	430.21	452.13	517.45
PCRh-3	254.28	412.12	447.19	510.53
PCRh-1,2	287.13	416.92	431.57	543.83
PCRh-2,2	273.63	412.47	428.68	535.32
PCRh-3,2	263.14	403.98	425.31	532.71

[a] T_i: Initial degradation temperature at 5% wt % loss, T_{50}: temperature at 50% wt % loss, T_{75}: temperature at 75% wt % loss, and T_{max}: degradation temperature at maximum wt % loss.

3.1.5. Thermogravimetric Analysis. Thermogravimetric analysis (TGA) was done for all of the samples to determine their degradation rate or thermal stability. Figure 9 and Table 2 show the studies of the TGA of PCR husk, LDPE, EPR/LDPE, and PCRh/EPR/LDPE composites. PCRh degrades in three stages and releases volatile substances at 100 °C. Due to Moisture loss, around 190 °C is when PCRh breakdown first begins. The LDPE and LDPE/EPR matrix shows only one deterioration phase. At about 368 and 336 °C, respectively, they begin to deteriorate. The degradation temperature of the EPR/LDPE blend was reduced due to the degradation of EPR at lower temperatures. Up to 100 °C, neither the PCRh/LDPE nor the PCRh/EPR/LDPE composites produce any volatile substances. Depending on the content of the composite, their deterioration starts in the temperature range of 252−265 °C. The temperature range between 511 and 523 °C, which is between the degradation temperatures of PCRh and LDPE, is where all composites degrade most significantly.

Due to the low quantity of degradable PCRh, the PCRh-1 composite with the lowest PCRh content exhibited the maximum thermal stability at the start of deterioration. Similarly, among all of the fabricated composites, composite PCRh-1,2 showed the least amount of heat deterioration. These studies concluded that as the fraction of husk loading increased, the thermal stability of all composites decreased.

The temperatures for every specimen are listed in Table 2 at different wt % reductions. Interestingly, considering the change in mechanical characteristics caused by the inclusion of the EPR coupling agent, all the composite specimen's thermal degradation temperatures continuously dropped. In PCRh-1, the T_i, T_{50}, T_{75}, and T_{max} temperatures are 304.04, 437.84, 455.91, and 523.29 °C, respectively. The composite's degradation temperature has lowered due to the inclusion of EPR. Table 2 reports the degradation temperature at various wt % for all composites. Composites PCRh-1, PCRh-2, PCRh-3, PCRh-1,2, PCRh-2,2, and PCRh-3,2 provided a residual mass of 0.19, 0.74, 1.55, 0.22, 0.48, and 1.157%, respectively, after full deterioration at 800 °C, which was comparable to PCRh and LDPE.

3.1.6. Differential Thermogravimetric Analysis. The differential thermogravimetric analysis (DTG) curves for LDPE, EPR/LDPE, and all composites are shown in Figure 10. PCRh, LDPE, and EPR/LDPE degradation showed maximum rates at 325, 403, and 408 °C, respectively. The husk DTG curves often showed a two-stage degradation process, with the first phase including the breakdown of hemicellulose and loss of

https://doi.org/10.1021/acsomega.3c07697
ACS Omega 2024, 9, 2740−2751

Table 3. Calculation of Crystallinity for All the Composites

LDPE	PCRh	EPR	sample	T_C (°C)	ΔH_m (J/g)	T_m (°C)	% crystallinity $X_c = \frac{\Delta H_m \times 100}{W_m \times \Delta H_m^0}$ ΔH_m^0 = 285 J/g
100	0	0	LDPE	109.38	**81.421**	**126.41**	28.56
90	0	10	EPR/LDPE	116.85	69.360	124.86	27.04
90	10	0	PCRh-1	115.52	66.791	127.49	26.03
80	20	0	PCRh-2	115.75	55.440	126.25	24.31
70	30	0	PCRh-3	109.18	47.213	127.03	23.66
80	10	10	PCRh-1,2	116.42	63.500	127.82	27.85
70	20	10	PCRh-2,2	116.89	45.016	126.96	22.56
60	30	10	PCRh-3,2	114.26	33.510	125.08	19.59

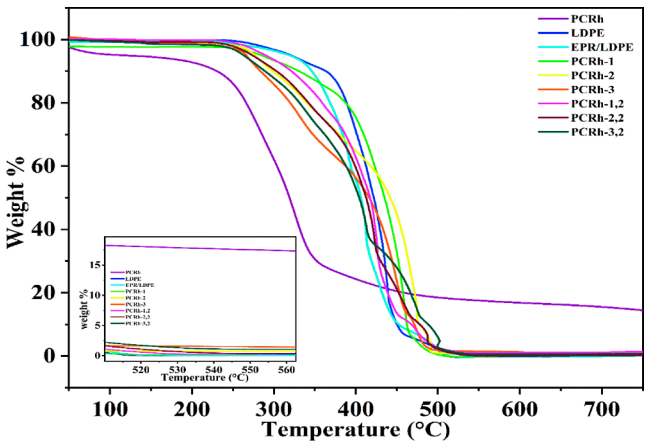

Figure 9. TGA graph of LDPE, the EPR/LDPE blend, and all various composites.

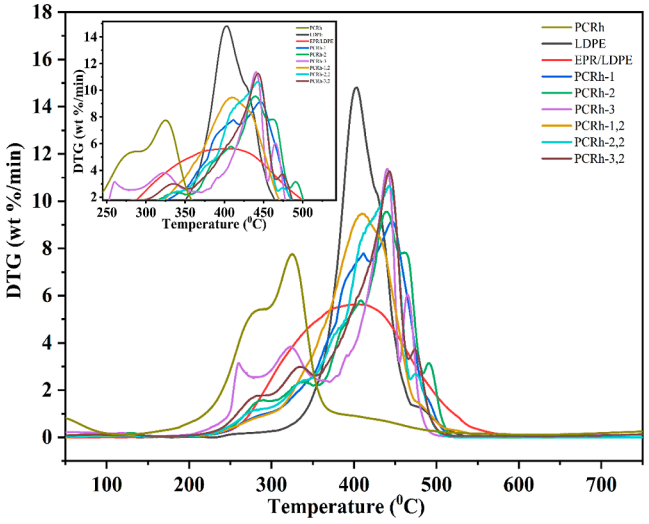

Figure 10. DTG graph of LDPE, EPR/LDPE blend, PCRh, and all of the various composites.

moisture and the second involving the depolymerization and breakdown of cellulose and lignin.[31,43,45] The deterioration of the husk continues at a significantly slower pace after the maximum weight loss occurs at the specified temperature. Like LDPE, EPR/LDPE degrades in a single step and at the fastest rate at temperatures of about 403.53 and 406.68 °C. The maximum rate of deterioration occurred at around 60% of the weight loss, which is supported by Figure 10. However, the deterioration of fibrous husk (I shoulder) and the breakdown of the polymer matrix were once more evident in the case of composites (II shoulders).

Similarly, the maximum rate of deterioration was shown at the II shoulder for the composites PCRh-1, PCRh-2, PCRh-3, PCRh-1,2, PCRh-2,2, and PCRh-3,2, which were recorded at 446.02, 439.42, 440.28, 410.36, 442.36, and 442.65 °C, respectively. It is interesting to note the greatest rate of deterioration in all composites tested with EPR. The formation of a strong interfacial contact between the PCRh and the polymer matrix may cause this noticeable increase in the composites' greatest rate of degradation when compared to both the PCRh and LDPE matrix.

3.1.7. Differential Scanning Calorimetry. DSC was used to examine the thermal behaviors of LDPE, EPR/LDPE, and all composite materials, including the crystallization temperature (T_c), melting point (T_m), heat of enthalpy (H_m), and percentage of crystallinity (X_c). Thermograms and crystallinity values for LDPE, EPR/LDPE, and all composites are shown in Figure 11 and Table 3, respectively. Similarly, the melting enthalpy is determined by the area under the melting temperature curve. The estimated crystallization temperature of LDPE was about 109.38 °C, while the T_c of EPR/LDPE was 116 °C, slightly higher than that of virgin LDPE. The peak and valley maxima of the thermogram indicate the temperature at which crystals form when frozen and melt when heated.

Most likely, the heterogeneous nucleation brought on by EPR particles caused the increase in the T_c of the EPR/LDPE blend. Additionally, all composites have observed T_c values of PCRh-1, PCRh-2, PCRh-3, PCRh-1,2, PCRh-2,2, and PCRh-3,2. Due to the heterogeneous nucleation caused by the presence of PCR husk, all of the composites once more reported better T_c values than the virgin LDPE. The melting points for PCRh-1, PCRh-2, PCRh-3, PCRh-1,2, PCRh-2,2, and PCRh-3,2 were reported to be 127.49, 126.25, 127.03, 127.82, 126.96, and 125.08 °C, respectively. It is fascinating to observe that the melting points of all the composites did not deviate significantly from virgin LDPE. Because the presence of reinforcements had a minimal effect on the T_m, it was assumed that the polymeric chains must have caused the composites to melt. The article was consistent with the findings of Maurya et al., who found no significant variation in the melting points of various composites.[46]

The enthalpy of melting (H_m) values for LDPE, EPR/LDPE, and PCRh-1, PCRh-2, PCRh-3, PCRh-1,2, PCRh-2,2, and PCRh-3,2 were observed as 81.421, 69.360, 66.791, 55.440, 47.213, 63.500, 45.016, and 33.510 J/g, respectively. Equation 1 was used to determine the percentage of crystallinity of LDPE, EPR/LDPE, and all composites. The values of X_c for LDPE, EPR/LDPE, and all composites are PCRh-1, PCRh-2, PCRh-3, PCRh-1,2, PCRh-2,2, and PCRh-3,2 were 28.56, 27.04, 26.03, 24.31, 23.66, 27.85, 22.56, and 19.59, respectively. It is interesting to observe that X_c was lower in

https://doi.org/10.1021/acsomega.3c07697
ACS Omega 2024, 9, 2740−2751

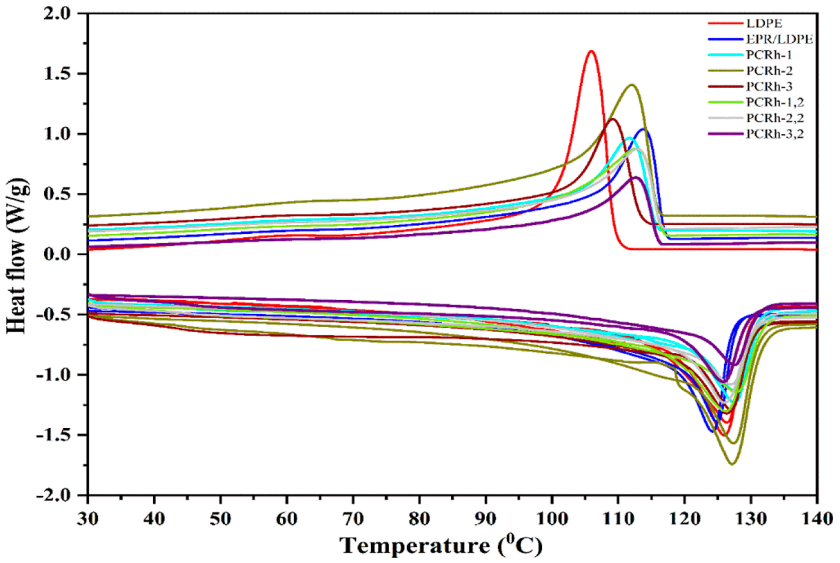

Figure 11. DSC graph of LDPE, the EPR/LDPE blend, and all various composites.

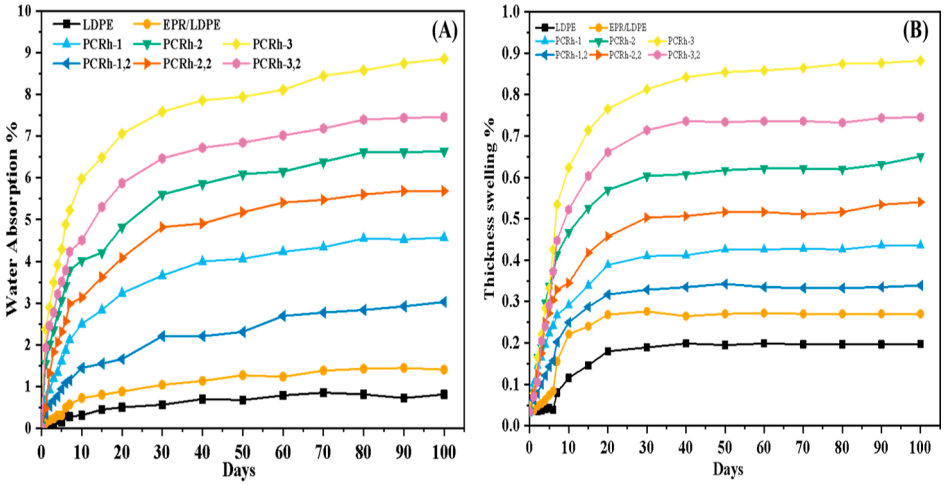

Figure 12. Analysis of water absorption test (A) and thickness swelling (B) of virgin LDPE, EPR/LDPE, and all polymer composites.

all the composites than in the virgin LDPE. The reinforcement of PCRh in the polymer matrix was responsible for the decrease in X_c of all the composites. It was hypothesized that the incorporation of foreign substances into the polymer matrix must have disrupted crystal development and formation.[25] Propylene reinforced with sunflower sanding sawdust also shows the decrease in % crystallinity of the composites.

3.1.8. Water Absorption Test. Water absorption tests of pristine LDPE and all manufactured composites were evaluated by storing all samples in closed containers filled with distilled water for >90 days. The increase in sample weight and sample thickness was recorded daily. LDPE and composites' weight change and thickness expansion were plotted as a function of days (Figure 12). It was found that the LDPE and LDPE/EPR blend samples absorbed the least amount of water after 90 days of water absorption. However, all composites reported greater water absorption characteristics than the basic matrix. Specimens LDPE, EPR/LDPE, PCRh-1, PCRh-2, PCRh-3, PCRh-1,2, PCRh-2,2, and PCRh-3,2 show a water absorption percentage of 0.91, 1.40, 4.57, 6.63, 8.85, 3.02, 5.69, and 7.46%, respectively. Similar results were obtained for thickness swelling, which showed percentages of swelling of 0.20, 0.29, 0.43, 0.65, 0.88, 0.33, 0.54, and 0.74% for the materials specimens LDPE, EPR/LDPE, PCRh-1, PCRh-2, PCRh-3, PCRh-1,2, PCRh-2,2, and PCRh-3,2, respectively. It is significant to observe that composites made by adding PCR husk reinforcement to an EPR/LDPE matrix had less water absorption than their LDPE-only counterparts. Potential interfacial development in the form of esters and hydrogen bonds at the PCRh−matrix interface seems to have reduced the water absorption properties of the EPR/LDPE composites. The presence of MAH increased the water absorption of the LDPE and EPR/LDPE blends. MAH caused molecular self-hydroxylation by environmental moisture. The results shown above were consistent with the information on sisal fiber-reinforced polypropylene and crown fiber reinforced with LDPE composites provided by Maurya et al. and Kumar et al.[12,25]

4. CONCLUSIONS

PCRh was successfully extracted from the pineapple crown waste and used to fabricate different composites containing LDPE and EPR. The addition of PCRh to the LDPE/EPR

https://doi.org/10.1021/acsomega.3c07697
ACS Omega 2024, 9, 2740−2751

composite significantly increased the tensile strength to 19.28 MPa as compared to pristine LDPE, EPR/LDPE composite having the tensile strength of 14.74 and 16.61 MPa, respectively. Substitution of virgin LDPE by PCRh/EPR/LDPE blends is possible because it offers greater mechanical strength and especially the flexural modulus compared with the virgin LDPE, so PCRh may work as a suitable plasticizer. The PCRh/EPR/LDPE blend can be applied in automotive applications, building materials, the electrical industry, aerospace sports, and office products. Since these composites have low specific gravity, relatively high strength, improved surface finish of molded composites, and moderately good mechanical properties, as compared to the synthetic fibers, they can be used in the automobile industry, particularly for interior vehicle components, including seat backs, boot liners, cargo shelves, front and rear door liners, truck liners, and door-trim panels.

AUTHOR INFORMATION

Corresponding Author

Chhaya Sharma − *Department of Paper Technology, Indian Institute of Technology Roorkee, Saharanpur 247001, India*; orcid.org/0000-0003-1148-7216; Email: chhaya.iitr@gmail.com, chhaya.sharma@pt.iitr.ac.in

Authors

Jitendra Kumar − *Department of Paper Technology, Indian Institute of Technology Roorkee, Saharanpur 247001, India*

Anuj Kumar − *Department of Paper Technology, Indian Institute of Technology Roorkee, Saharanpur 247001, India*

Atul Kumar Maurya − *National Institute for Materials Advancement, Pittsburg State University, Pittsburg, Kansas 66762-7500, United States*

Hariome Sharan Gupta − *Department of Polymer and Process Engineering, Indian Institute of Technology Roorkee, Saharanpur 247001, India*

Surendra Pal Singh − *Department of Paper Technology, Indian Institute of Technology Roorkee, Saharanpur 247001, India*

Complete contact information is available at: https://pubs.acs.org/10.1021/acsomega.3c07697

Author Contributions

JK contributed to analysis, writing, reviewing—draft, and methodology; **AK** contributed to formal analysis and methodology, and writing; **AKM** contributed to data curation, methodology, and validation; **HSG** contributed to formal analysis; **SPS** contributed to supervision, review, and editing; and **CS** contributed to conceptualization, resources, funding, review and editing, and supervision.

Funding

The work was financially supported by the Ministry of Education (MoE), Government of India, India, and the Indian Institute of Technology, Roorkee, India.

Notes

The authors declare no competing financial interest.

This study does not involve any study related to animal/human testing for completing this research.

ACKNOWLEDGMENTS

The authors are very grateful to the Ministry of Education (MoE), Government of India, India, for financial support and Indian Institute of Technology Roorkee, India, for providing the characterization facility and other resources.

REFERENCES

(1) Rosli, N. A.; Wan Ishak, W. H.; Ahmad, I. Eco-Friendly High-Density Polyethylene/Amorphous Cellulose Composites: Environmental and Functional Value. *J. Clean. Prod.* **2021**, *290*, 125886.

(2) Siddharth, J. V.; Lawrence, I. D.; Jayabal, S. Mechanical Behavior of Raavi and Pineapple Fiber-Reinforced Hybrid Polyester Composites. In *Lecture Notes in Mechanical Engineering*; Vijayan, S., Subramanian, N., Sankaranarayanasamy, K., Eds.; Springer: Singapore, 2021; pp 227−238.

(3) Mulenga, T. K.; Ude, A. U.; Vivekanandhan, C. Techniques for Modelling and Optimizing the Mechanical Properties of Natural Fiber Composites: A Review. *Fibers* **2021**, *9* (1), 6−17.

(4) Gebremedhin, N.; Rotich, G. K. Manufacturing of Bathroom Wall Tile Composites from Recycled Low-Density Polyethylene Reinforced with Pineapple Leaf Fiber. *Int. J. Polym. Sci.* **2020**, *2020*, 1−9.

(5) Ovalı, S.; Sancak, E. Investigation of Mechanical Properties of Jute Fiber Reinforced Low Density Polyethylene Composites. *https://doi.org/10.1080/15440478.2020.1838999* **2022**, *19*, 3109−3126.

(6) Ganesan, S.; Hemanandh, J.; Raja, K. S. S.; Purusothaman, M. Experimental Investigation and Characterization of HDPE & LDPE Polymer Composites. *Lect. Notes Mech. Eng.* **2021**, *23*, 785−799.

(7) Zong, G.; Hao, X.; Hao, J.; Tang, W.; Fang, Y.; Ou, R.; Wang, Q. High-Strength, Lightweight, Co-Extruded Wood Flour-Polyvinyl Chloride/Lumber Composites: Effects of Wood Content in Shell Layer on Mechanical Properties, Creep Resistance, and Dimensional Stability. *Journal of Cleaner Production.* **2020**, *244*, 118860.

(8) Gogoi, R.; Maurya, A. K.; Manik, G. A Review on Recent Development in Carbon Fiber Reinforced Polyolefin Composites. *Compos. Part C Open Access* **2022**, *8*, 100279.

(9) Hejna, A.; Przybysz-Romatowska, M.; Kosmela, P.; Zedler, Ł.; Korol, J.; Formela, K. Recent Advances in Compatibilization Strategies of Wood-Polymer Composites by Isocyanates. *Wood Sci. Technol.* **2020**, *54* (5), 1091−1119.

(10) Saha, A.; Kumar, S.; Kumar, A. Influence of Pineapple Leaf Particulate on Mechanical, Thermal and Biodegradation Characteristics of Pineapple Leaf Fiber Reinforced Polymer Composite. *J. Polym. Res.* **2021**, *28* (2), 66.

(11) Chowdhury, I. H.; Abdelwahab, M. A.; Misra, M.; Mohanty, A. K. Sustainable Biocomposites from Recycled Bale Wrap Plastic and Agave Fiber: Processing and Property Evaluation. *ACS Omega* **2021**, *6* (4), 2856−2864.

(12) Maurya, A. K.; Gogoi, R.; Manik, G. Study of the Moisture Mitigation and Toughening Effect of Fly-ash Particles on Sisal Fiber-Reinforced Hybrid Polypropylene Composites. *J. Polym. Environ.* **2021**, *29* (7), 2321−2336.

(13) Maurya, A. K.; Gogoi, R.; Manik, G. Mechano-Chemically Activated Fly-Ash and Sisal Fiber Reinforced PP Hybrid Composite with Enhanced Mechanical Properties. *Cellulose* **2021**, *28*, 8493−8508.

(14) Maurya, A. K.; Gogoi, R.; Manik, G. Study of Effect of Multiple Recycling on the Mechanical Properties of Sisal Fiber and Fly Ash Reinforced Hybrid Composites. In *Fifth International Conference on Reuse and Recycling of Materials (ICRM-2020)*; Krispon: Kottayam, 2021; Vol. *1*, pp 26.

(15) Maurya, A. K.; Gogoi, R.; Manik, G. Sisal Fiber/Fly Ash Reinforced Hybrid Polypropylene Composite: An Investigation into the Thermal, Rheological and Crystallographic Properties. In *2nd International Congress on Advances in Mechanical and System Engineering (CAMSE 2021)*; Manik, G., Kalia, S., Sahoo, S. K., Sharma, T. K., Verma, O. P., Eds.; Springer Singapore: Jalandhar, India, 2021.

(16) Prasad, N.; Agarwal, V. K.; Sinha, S. Banana Fiber Reinforced Low-Density Polyethylene Composites: Effect of Chemical Treatment and Compatibilizer Addition. *Iran. Polym. J. (English Ed.* **2016**, *25* (3), 229−241.

(17) Todkar, S. S.; Patil, S. A. Review on Mechanical Properties Evaluation of Pineapple Leaf Fibre (PALF) Reinforced Polymer Composites. *Compos. Part B Eng.* **2019**, *174*, 106927.
(18) Maurya, A. K.; Gogoi, R.; Sethi, S. K.; Manik, G. A Combined Theoretical and Experimental Investigation of the Valorization of Mechanical and Thermal Properties of the Fly Ash-Reinforced Polypropylene Hybrid Composites. *J. Mater. Sci.* **2021**, *56* (30), 16976−16998.
(19) Saha, A.; Kumar, S.; Zindani, D.; Bhowmik, S. Micro-Mechanical Analysis of the Pineapple-Reinforced Polymeric Composite by the Inclusion of Pineapple Leaf Particulates. *Proc. Inst. Mech. Eng. Part L J. Mater. Des. Appl.* **2021**, *235* (5), 1112−1127.
(20) Alim, A. A. A.; Baharum, A.; Shirajuddin, S. S. M.; Anuar, F. H. Blending of Low-Density Polyethylene and Poly(Butylene Succinate) (LDPE/PBS) with Polyethylene-Graft-Maleic Anhydride (PE-g-MA) as a Compatibilizer on the Phase Morphology, Mechanical and Thermal Properties. *Polymers (Basel).* **2023**, *15* (2), 261.
(21) Bumbudsanpharoke, N.; Wongphan, P.; Promhuad, K.; Leelaphiwat, P.; Harnkarnsujarit, N. Morphology and Permeability of Bio-Based Poly(Butylene Adipate-Co-Terephthalate) (PBAT), Poly(Butylene Succinate) (PBS) and Linear Low-Density Polyethylene (LLDPE) Blend Films Control Shelf-Life of Packaged Bread. *Food Control* **2022**, *132*, 108541.
(22) Horikawa, Y.; Hirano, S.; Mihashi, A.; Kobayashi, Y.; Zhai, S.; Sugiyama, J. Prediction of Lignin Contents from Infrared Spectroscopy: Chemical Digestion and Lignin/Biomass Ratios of Cryptomeria Japonica. *Appl. Biochem. Biotechnol.* **2019**, *188* (4), 1066−1076.
(23) Johny, V.; Mani, A. K.; Palanisamy, S.; Rajan, V. K.; Palaniappan, M.; Santulli, C. Extraction and Physico-Chemical Characterization of Pineapple Crown Leaf Fibers (PCLF). *Fibers 2023, Vol. 11, Page 5* **2023**, *11* (1), 5.
(24) Reichert, A. A.; de Sá Cesar Augusto, R.; Beatrice, M. G.; Fajardo, r.; de Oliveira, A. D.; Fajardo, A. R.; de Oliveira, A. D. Utilization of Pineapple Crown Fiber and Recycled Polypropylene for Production of Sustainable Composites. *J. Renew. Mater.* **2020**, *8* (10), 1327−1341.
(25) Kumar, J.; Maurya, A. K.; Gupta, H. S.; Singh, S. P.; Sharma, C. Development of Eco-Friendly Bio-Composite by Reinforcing Pineapple Fruit Waste Crown Fiber to Ethylene-Propylene Rubber Modified Polyethylene. *Polym. Compos.* **2022**, *43* (11), 8259−8273.
(26) Al-Malaika, S.; Kong, W. Reactive Processing of Polymers: Effect of in Situ Compatibilisation on Characteristics of Blends of Polyethylene Terephthalate and Ethylene-Propylene Rubber. *Polymer (Guildf).* **2005**, *46* (1), 209−228.
(27) Rajandas, H.; Parimannan, S.; Sathasivam, K.; Ravichandran, M.; Su Yin, L. A Novel FTIR-ATR Spectroscopy Based Technique for the Estimation of Low-Density Polyethylene Biodegradation. *Polym. Test.* **2012**, *31* (8), 1094−1099.
(28) Malkapuram, R.; Kumar, V.; Negi, Y. S. Recent Development in Natural Fiber Reinforced Polypropylene Composites. *J. Reinf. Plast. Compos.* **2009**, *28* (10), 1169−1189.
(29) Kumar, P.; Singh, J.; Kumari, N.; Jurail, S. S.; Verma, D.; Maurya, A. K. Study of Mechanical and Thermal Behavior of Alkali Modified Groundnut Shell Powder Reinforced ABS Composites. *Polym. Compos.* **2022**, *43* (7), 4569−4587.
(30) Abdelmouleh, M.; Boufi, S.; Belgacem, M. N.; Dufresne, A. Short Natural-Fibre Reinforced Polyethylene and Natural Rubber Composites: Effect of Silane Coupling Agents and Fibres Loading. *Compos. Sci. Technol.* **2007**, *67* (7−8), 1627−1639.
(31) Dikobe, D. G.; Luyt, A. S. Thermal and Mechanical Properties of PP/HDPE/Wood Powder and MAPP/HDPE/Wood Powder Polymer Blend Composites. *Thermochim. Acta* **2017**, *654* (April), 40−50.
(32) Chun, K. S.; Husseinsyah, S.; Syazwani, N. F. Properties of Kapok Husk-Filled Linear Low-Density Polyethylene Ecocomposites. *J. Thermoplast. Compos. Mater.* **2016**, *29* (12), 1641−1655.
(33) Ou, R.; Xie, Y.; Wolcott, M. P.; Sui, S.; Wang, Q. Morphology, Mechanical Properties, and Dimensional Stability of Wood Particle/High Density Polyethylene Composites: Effect of Removal of Wood Cell Wall Composition. *Mater. Des.* **2014**, *58*, 339−345.
(34) Marin, D.; Chiarello, L. M.; Wiggers, V. R.; Oliveira, A. D. d.; Botton, V. Effect of Coupling Agents on Properties of Vegetable Fiber Polymeric Composites: Review. *Polimeros* **2023**, *33* (1), 13−16.
(35) Fan, M.; Dai, D.; Huang, B. Fourier Transform Infrared Spectroscopy for Natural Fibres. *Fourier Transform—Mater. Anal.* **2012**, *3* (May 2012), 45.
(36) Essoua, G. G. E.; Blanchet, P.; Landry, V.; Beauregard, R. Maleic Anhydride Treated Wood: Effects of Drying Time and Esterification Temperature on Properties. *BioResources* **2015**, *10* (4), 6830−6860.
(37) Fakhrul, T.; Mahbub, R.; Islam, M. A. Properties of Wood Sawdust and Wheat Flour Reinforced Polypropylene Composites Fakhrul, Mahbub and Islam. *J. Mod. Sci. Technol.* **2013**, *1* (1), 135−148.
(38) Janardhnan, S.; Sain, M. Isolation of Cellulose Nanofibers: Effect of Biotreatment on Hydrogen Bonding Network in Wood Fibers. *Int. J. Polym. Sci.* **2011**, *2011*, 1−6.
(39) Kallakas, H.; Martin, M.; Goljandin, D.; Poltimäe, T.; Krumme, A.; Kers, J. Mechanical and Physical Properties of Thermally Modified Wood Flour Reinforced Polypropylene Composites. *Agron. Res.* **2016**, *14* (January), 994−1003.
(40) Singh, J. K.; Rout, A. K. Thermal Stability and Dynamic Mechanical Analysis of Nano-Biofillers Blended Hybrid Composites Reinforced by Cellulosic Borassus Flabellifer L. Fiber. *Int. J. Polym. Anal. Charact.* **2023**, *28* (6), 552−563.
(41) Mouhoub, O. A.; Rouabah, F.; Fois, M.; Haddaoui, N. Characterization of Cellulose Acetate/Low Density Polyethylene Fibre Reinforced Composite. *J. Adhes. Sci. Technol.* **2023**, *37* (23), 3358−3378.
(42) Kelly-Walley, J.; Ortega, Z.; McCourt, M.; Millar, B.; Suárez, L.; Martin, P. Mechanical Performance of Rotationally Molded Multilayer MLDPE/Banana-Fiber Composites. *Materials (Basel).* **2023**, *16* (20), 6749.
(43) Abhilash, S. S.; Jeesmon, K. C.; Singaravelu, D. L. Influence of Rice Husk Particles on Mechanical and Vibration Damping Characteristics of Roto-Molded Polyethylene Composites. *Fibers Polym.* **2023**, *24* (2), 355−359.
(44) Gupta, M. K. Effect of Variation in Frequencies on Dynamic Mechanical Properties of Jute Fibre Reinforced Epoxy Composites. *J. Mater. Environ. Sci.* **2018**, *9* (1), 100−106.
(45) Reichert, A. A.; Sá, M. R.; Castilhos de Freitas, T.; Barbosa, R.; Alves, T. S.; Backes, E. H.; Alano, J. H.; Oliveira, A. D. Barrier, Mechanical and Morphological Properties of Biodegradable Films Based on Corn Starch Incorporated with Cellulose Obtained from Pineapple Crowns. *J. Nat. Fibers* **2021**, *19* (14), 8541−8554.
(46) Maurya, A. K.; Gogoi, R.; Manik, G. Thermal Behavior of Elastomer Blends and Composites. In *Elastomer Blends and Composites*; Rangappa, S. M., Parameswaranpillai, J., Siengchin, S., Ozbakkaloglu, T., Eds.; Elsevier, 2022; pp 149−169.

https://doi.org/10.1021/acsomega.3c07697
ACS Omega 2024, 9, 2740−2751